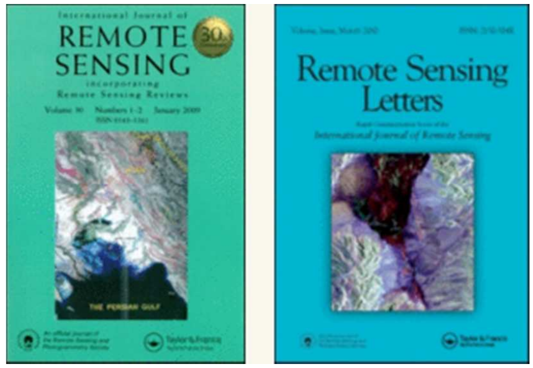

Markovian modelling and Fisher distribution for unsupervised segmentation of radar images

Journal:	*International Journal of Remote Sensing*
Manuscript ID:	TRES-PAP-2011-0779.R2
Manuscript Type:	IJRS Research Paper
Date Submitted by the Author:	27-Feb-2013
Complete List of Authors:	Benboudjema, Dalila; Telecom SudParis, CITI Tupin, Florence; Telecom Paris Tech, TSI
Keywords:	IMAGE PROCESSING, MODELLING
Keywords (user defined):	Hidden Markov fields, triplet Markov fields, non stationary modelling, Fisher distribution, Mellin Transform, iterative conditional estimation, maximum posterior mode, unsupervised segmentation, texture classification, synthetic aperture radar (SAR) images

Markovian modelling and Fisher distribution for unsupervised classification of radar images

[1]Dalila Benboudjema and [2]Florence Tupin

[1]Institut Telecom, Telecom SudParis, CNRS UMR 5157
9, rue Charles Fourier, 91000 Evry, France

[2]Institut Telecom, Telecom Paris Tech, Département TSI, CNRS UMR 5141
46, rue Barrault, 75013 Paris, France

Abstract

Statistical segmentation techniques based on hidden Markov field (HMF) modelling have retained considerable interest in the past years. They take the contextual information into account, in a particularly elegant and rigorous way. Although these models have been thoroughly tested, they can fail in some cases such as the non stationary one. In this paper we propose to consider the recently developed triplet Markov field (TMF), which models non stationary images, and to use the Fisher distribution, which is adapted to a wide range of surfaces, for modelling the SAR image noise. Examples illustrate the difference between the approach we propose and classical ones. Different experiments indicate that the new model and its associated unsupervised algorithm perform better than classical ones.

Index terms Hidden Markov fields, triplet Markov fields, non stationary modelling, Fisher distribution, Mellin Transform, iterative conditional estimation, maximum posterior mode, unsupervised segmentation, texture classification, synthetic aperture radar (SAR) images.

I. INTRODUCTION

There are nowadays many SAR satellite sensors (such as TerraSAR-X, RADARSAT-2, CosmoSkyMed) regularly acquiring radar data. Although such sensors are very popular due to their all-weather and all-time capabilities, SAR data remain difficult to interpret due to speckle phenomenon (coherent imagery) and geometrical distortions (Goodman, 1976). For many applications, segmentation or classification is a preliminary step to further processing, such as scene interpretation (Fjortoft et al. 2003, Pellizzeri et al. 2003, Marques et al. 2012) or interferometric 3D reconstruction (Tison et al. 2007).

In this paper, we present a new unsupervised classification method dedicated to SAR images, especially to the case of high resolution images and urban areas. This application is of major interest with the increasing improvement of sensor resolutions and the environmental applications linked to cities development and urban survey. The proposed approach, which is compared to classical classification Markovian methods (Delignon et al. 1997, Fjortoft *et al.*, 2003), is based on two recent models.

First, the triplet Markov fields (TMF), which generalize the classical hidden Markov fields (HMFs) (Geman and Geman 1984; Guyon, 1995; Marroquin et al., 1987; Pérez, 1998; Winkler 2003; Won and Gray, 2004) are used (Benboudjema and Pieczynski, 2005; Benboudjema and Pieczynski, 2007). One of the main interests of this triplet model is that it is able to take into account different local interactions in the image. In the classical Markov field context, the prior distribution of the Hidden Field is defined by some functions specified on cliques; a field will be considered stationary when these functions do not depend on the position of the cliques in the image. Roughly speaking, in the stationary images the visual aspect of the spatial organization of different labels is almost independent of pixel position. The triplet model introduces a third field, controlling the local interaction in the image and thus allowing a kind of non-stationarity for the model.

The second innovation is linked to the data distributions (likelihood term). In (Nicolas, 2006), a new model for SAR images has been proposed. It is based on log-statistics and Mellin transform, and suggests the use of Fisher distributions to model high resolution SAR images. The interest of this distribution compared to classical SAR distributions such as Gamma (Lopes et al. 1990), K (Nezry et al. 1996, Oliver, 1984) Weibull (Kuruoglu and Zerubia, 2004) or Pearson system (Delignon et al., 1997) is its capability of modelling a wide range of surfaces (natural surfaces such as vegetation but also man-made structures, frequently observed in urban areas) (Gao 2010). Another choice could have been the Generalized Gamma distribution (Voisin et al. 2012, Marques et al. 2012) which is rather close to Fisher. Compared to the work presented in (Tison et al. 2007), here a fully unsupervised framework is developed and instead of HMF, TMF are investigated.

This paper is based on previous works on triplet model (Benboudjema and Pieczynski 2005) and statistical modelling of radar distributions (Tison et al. 2004). It is an extension of the work published in (Benboudjema et al. 2007) and focuses on two aspects of the proposed approach: a better justification of the interest of the Fisher distribution and the triplet model for SAR urban areas; a more detailed description of the algorithm with practical information for implementation.

This paper is organized as follows. In Section II we present the triplet Markov field (TMF) model. Section III is devoted to Fisher distribution and second kind statistics. In Section IV we briefly recall the parameter estimation procedure and give the full scheme of this approach with practical information for implementation. Examples of segmentation are provided in Section V. A comparison study shows the improvements brought by the original aspects (TMF and Fisher) of our approach. Finally, conclusion and perspectives are reported in Section VI.

II. TRIPLET MARKOV FIELD

Let S be the set of pixels, $X=(X_s)_{s\in S}$ and $Y=(Y_s)_{s\in S}$ two random fields defined on S. Each X_s takes its values in a finite set of classes $\Omega=\{\omega_1,...,\omega_K\}$, whereas each Y_s takes its values in the set of positive real numbers R^+. X is the hidden "label" field, while Y is the observed field. In the context of this paper, realizations of Y are the SAR amplitudes. Thus the problem is to estimate the hidden realization of Y from the observed realization of X. Besides these two processes defined in a classical Markov field (HMF), and in order to model some kind of "non stationary" Markov field, we have introduced a third process $U=(U_s)_{s\in S}$, which represents the field of "stationarities". Each U_s takes its values in a finite set $\Lambda=\{\lambda_1,...,\lambda_M\}$ which is the set of the possible kinds of local interactions. For each λ_i value, a set of parameters modeling the local interactions is associated (see an example below). These values will be denoted by "stationarities" in the following meaning that they govern the local interactions.

We then assume that the couple (X,U) is Markovian. The problem remains the same as in a classical case i.e. estimate the unobservable realizations $X=x$ from the observed one $Y=y$. Let us put $\Lambda=\{a,b\}$ -in our experiments we limit ourselves to two "stationarities" but an extension to more than two stationarities does not raise any problem- and let us consider that the couple (X,U) is a Markov field, then the distribution $p(x,u)$ is written:

$$P(x,u)=\gamma\exp[-W(x,u)] \tag{2.1}$$

With $W(x,u)=\sum_{(s,t)\in C}W_c(x_s,x_t,u_s,u_t)$ if we consider a Markov random field with order 2 interaction, W_c denoting the potential of the clique (here, a pair of neighboring pixels). In this paper, we will consider the following model with horizontal c_H and vertical c_V clique potentials:

$$W_{cH}(x_s,x_t,u_s,u_t)=\alpha_H^1(1-2\delta(x_s,x_t))-(\alpha_{aH}^2\delta*(u_s,u_t,a)+\alpha_{bH}^2\delta*(u_s,u_t,b))(1-\delta(x_s,x_t))$$
$$W_{cV}(x_s,x_t,u_s,u_t)=\alpha_V^1(1-2\delta(x_s,x_t))-(\alpha_{aV}^2\delta*(u_s,u_t,a)+\alpha_{bV}^2\delta*(u_s,u_t,b))(1-\delta(x_s,x_t)) \quad (2.2)$$

With $\delta(x_s,x_t)=1$ for $x_s=x_t$, and 0 otherwise, $\delta*(a,b,c)=1$ for $a=b=c$, and $\delta*(a,b,c)=0$ otherwise. c_H is the set of couples of pixels which are horizontally neighbours and C_V is the set of couples of pixels vertically neighbours. If we consider a clique of two pixels, the model will lead to different potentials, depending on the values of x_s and x_t (the labels of the pixels), but also depending on their related "stationarities" u_s and u_t. It thus introduces another control on the clique potentials thanks to the U values. This model can be seen as a generalized Potts model. If we take a simple example where $x_s \neq x_t$, we still have three possible potentials depending if $u_s=u_t=a$, or $u_s=u_t=b$, or $u_s \neq u_t$; the associated potentials are respectively $\alpha_H^1-\alpha_{Ha}^2$, $\alpha_H^1-\alpha_{Hb}^2$ or α_H^1. It implies a larger variety of configurations introduced by the "stationarity" values. For the sake of simplicity, the models used in the following are only defined for two "stationarity" values and with parameters for horizontal and vertical cliques (we will see later how they are estimated).

Therefore, this additional process U allows the detection of different "stationarities" in the image. To be able to handle the posterior field, we need some assumptions. First, the random variables Y_s are assumed to be independent conditionally on X and U, and that the distribution of each Y_s conditionally on $(X=x,U=u)$ is equal to its distribution conditionally on $X_s=x_s$ (this is justified for uncorrelated SAR data). Let us note that a more complicated model could be used to introduce a dependency on both x_s and u_s. We have with these assumptions:

$$P(y|x,u)=\prod_{s\in S}P(y_s|x_s) \quad (2.3)$$

The distribution $p(x,u,y)$ is then given by:

$$\begin{aligned}P(x,u,y)&=P(x,u)P(y|x,u)\\&=\gamma\exp\left[-W(x,u)+\sum_{s\in S}Log(p(y_s|x_s))\right]\end{aligned} \quad (2.4)$$

which is still Markovian. Denoting by V_s the neighborhood of pixel s, it is thus possible to compute the local conditional probabilities $P\left((x_s,u_s)=(\omega_i,\lambda_j)\middle|y,x_t,u_t,t\in V_s\right)$ by computing the local energy $-\log(p(y_s|x_s))+\sum_{(s,t)\ /\ s\in c} W_c(x_s,x_t,u_s,u_t)$ for a given configuration of the neighboring pixels, and a known value of the observation y_s (as for usual Markov random field, except that the number of conditional probabilities increases due to the possibilities for the u_s values). Since it is possible to compute the local conditional probabilities, a Gibbs Sampler can be used to draw (x_s,u_s) samples and estimate the probabilities $P\left((x_s,u_s)=(\omega_i,\lambda_j)\middle|y\right)$.

For a classification problem, different solutions for X and U can be searched for: Maximum A Posteriori Solution (called MAP, with an optimization done by Simulated Annealing) or Maximum Posterior Mode (MPM, relying on the sampling of data following the posteriori distribution) which takes the most frequent values for the label field and the "stationarity" field in each pixel.

One can calculate $P(x_s=\omega_i|y)$, as well as $P(u_s=\lambda_j|y)$, by:

$$P(x_s=\omega_i|y)=\sum_{u\in\Lambda}P(x_s=\omega_i,u_s=\lambda_j|y) \tag{2.5}$$

$$P(u_s=\lambda_j|y)=\sum_{x\in\Omega}P(x_s=\omega_i,u_s=\lambda_j|y) \tag{2.6}$$

And select the most probable values for each pixel. This estimator (MPM) is used due the parameter estimation method that we will describe in section IV (instead of the MAP estimator).

In conclusion, this model allows us to extract both fields, namely the hidden field X and the field U which models different stationarities of X. Indeed, when we are interested in the different "stationarities" of the image without taking care of classes, we will focus on the U field, and when we look for labels we will focus on the X field.

The problem of the definition of the data attachment term is addressed in the next session for SAR images, and the method for the clique potential estimation is described in section IV, as well as the details of implementation of the proposed method.

III. SECOND KIND STATISTICS AND FISHER DISTRIBUTION

3.1 Mellin transformation and Fisher distribution

The Fisher distribution is quite well suited for SAR images processing since it is a good model for many kinds of surfaces: urban objects, vegetation, textured areas, etc. Instead of using many different distributions as in (Delignon et al., 1997) a single one (Fisher) is introduced. Indeed, recent studies (Tison et al. 2004; Tison et al., 2007, Gao 2010) have shown that Fisher distributions are well adapted for SAR images in urban areas (instead of Gamma pdf –exponential decay- having tail behavior at high gray level values). To provide good estimates of the parameters, one has to use second kind statistics defined by Mellin transform (MT) (Nicolas, 2006). Let us recall what MT is and how one can use it to estimate the parameters of Fisher distribution.

Let us consider a function f defined on R^+, the MT of f noted as $MT[f]$ is written as :

$$MT[f](s) = \int_0^{+\infty} v^{s-1} f(v) dv \tag{3.1}$$

where s is a complex number. As probability density functions (pdf) of amplitude images are defined over this interval, the use of MT is possible. Let us notice that the latter has a relationship with the Fourier Transform (*FT*). Indeed, the characteristic function of the function f is the Fourier Transform of its pdf, the n^{th} moment is the n^{th} derivate of the characteristic function and the cumulants are the n^{th} derivatives of the characteristic function logarithm, which allow the deduction of the second kind statistics (Gradshteyn and Rayzhik, 2000). The latter are defined as follows:

- Second-kind first characteristic function:

$$\phi_x(s) = MT[p(y|x)] = \int_0^{+\infty} y^{s-1} p(y|x) dy \tag{3.2}$$

- Second-kind second characteristic function:

$$\psi_x(s) = \log(\phi_x(s)) \tag{3.3}$$

- Second-kind r^{th} order characteristic moment (or log-moment):

$$\tilde{m}_r = \left. \frac{d^r \phi_x(s)}{ds^r} \right|_{s=1} \tag{3.4}$$

- Second-kind r^{th} order characteristic cumulant (or log-cumulant):

$$\tilde{k}_r = \left. \frac{d^r \psi_x(s)}{ds^r} \right|_{s=1} \tag{3.5}$$

Although it is beyond the scope of this paper to detail the use of the Mellin transform for SAR data, these second-kind statistics provide useful tools to handle the distributions encounter with SAR images (Nicolas 2006).

Among the distribution that are useful to model the different areas that can be encountered in a SAR image, the Fisher distribution is quite popular due to its “genericity”, being able to model either homogeneous areas (such as ground) or heterogeneous ones (such as urban areas).

The Fisher distribution for amplitude is given by (Nicolas 2006):

$$F_A(\mu, L, M) = \frac{\Gamma(L+M)}{\Gamma(L)\Gamma(M)} \sqrt{\frac{L}{M}} \frac{2}{\mu} \frac{\left(\sqrt{\frac{L}{M}} \frac{y}{\mu}\right)^{2L-1}}{\left(1+\left(\sqrt{\frac{L}{M}} \frac{y}{\mu}\right)^2\right)^{L+M}}, \qquad M > L \tag{3.6}$$

where $\Gamma(.)$ is the Gamma function, μ is the mean and L, M are form parameters. The second kind characteristic function is then written as:

$$\phi_F(s) = \mu^{s-1} \frac{\Gamma\left(L + \frac{s-1}{2}\right)}{L^{\frac{s-1}{2}} \Gamma(L)} \frac{\Gamma\left(M + \frac{1-s}{2}\right)}{M^{\frac{1-s}{2}} \Gamma(M)}, \tag{3.7}$$

These parameters and specially (L, M)characterize the head and tail of the Fisher distribution.

3.2 Parameter estimation from complete data

There are many methods for parameter estimation, as moment method, maximum likelihood method, and log-moment method. As far as log-moments are concerned, there are links between log-cumulants $\tilde{k}_r$ and Fisher’s parameters (μ, L, M). These links are given by (Tison et al. 2007):

$$\begin{aligned} \tilde{k}_1 &= \log(\mu) + \frac{1}{2}(\Psi(L) - \log(L) - (\Psi(M) - \log(M))) \\ \tilde{k}_2 &= \frac{1}{4}(\Psi(1, L) + \Psi(1, M)) \\ \tilde{k}_3 &= \frac{1}{8}(\Psi(2, L) - \Psi(2, M)) \end{aligned} \tag{3.8}$$

where Ψ is a Polygamma function. Besides, the log-cumulants $\tilde{k}_r$ can be empirically estimated by (they are equal to the log-moments for r<3):

$$\tilde{k}_1 = \mathrm{E}[(\log(y))] \tag{3.9}$$

$$\tilde{k}_r = \mathrm{E}\left[\left(\log(y) - \tilde{k}_1\right)^r\right], \; r > 1 \tag{3.10}$$

Although this is not the subject of this paper, it can be shown that the log-moment method is more accurate, in terms of the variance of estimators, than the moment method (Nicolas, 2006). Besides, the maximum likelihood method is not always numerically tractable, whereas the log-moment is computationally efficient. For these reasons, we have used the log-moments method to estimate Fisher's parameters (Tison et al. 2004).

We will see in the next section how the triplet random fields and Fisher distribution with parameter estimation by log-cumulant can be used to define an unsupervised segmentation algorithm for SAR images.

IV. THE UNSUPERVISED SEGMENTATION ALGORITHM

4.1 Parameter estimation with ICE

As previously mentioned, our goal is to estimate the hidden field X from the observed one $Y = y$. In other words, having a noisy SAR image y, we try to recover the segmented image $\hat{x}$ so that it will be as close as possible to the ground truth x. Obviously, this kind of processing can not be possible without knowledge of the model parameter.

We need the estimation of two kind of parameters. First, we need the estimation the parameters of the data attachment term (or log-likelihood $-\log(p(y_s | x_s))$) which is the link between the observed amplitude value in the SAR image y_s and the label value x_s that we affect to the pixel s. As described in the previous section, we propose to use a Fisher distribution for this term and we thus need to estimate the (μ, L, M) for each class we consider. In this paper, the number of classes will be manually fixed by the user. Second, we need the estimation of the clique potentials $W_c(x_s, x_t, u_s, u_t)$ which (in our model) depends on the 6 parameters $\alpha = (\alpha_H^1, \alpha_V^1, \alpha_{aH}^2, \alpha_{aV}^2, \alpha_{bH}^2, \alpha_{bV}^2)$ as defined in equation (2.2).

Let us denote by θ the vector of parameters (in our case, the size of this vector is 3K+6, if K is number of classes). Different general parameter estimation methods can be used (McLachlan and Krishnan, 1997; Pérez, 1998) for this purpose. In our work we have used the iterative conditional estimation (ICE) method (Pieczynski 1992). This one seems to be well adapted to Markov fields context, providing good results in different situations (Delignon et al. 1997, Mignotte et al. 2000; Reed et al. 2003, Fjortoft et al. 2003).

The principle of ICE is as follows for two fields X and Y (the extension to the triplet is straightforward, X being replaced by (X,U)): we consider $\hat{\theta} = \hat{\theta}(X,Y)$ an estimation of θ from the complete data (X,Y) (we will precise in the following this estimation step in our application). X being unknown, we have to approximate $\hat{\theta} = \hat{\theta}(X,Y)$ by a function of Y.

The best approximation, as far as the mean squares error is concerned, is the conditional expectation. By denoting E_{θ_n} the conditional expectation based on the current parameter θ_n, ICE is written as:

i. Initialize $\theta = \theta_0$;

ii. $\theta_{n+1} = E_{\theta_n}[\hat{\theta}(X,Y) | Y = y]$

When the conditional expectation cannot be computed in a closed form, we simulate (e.g. by a Gibbs sampler) m realizations $x^1,...,x^m$ of X according to its distribution conditionally on $Y = y$ (called the posterior distribution) based on θ_n, and estimate the updated parameter with $\theta_{n+1} = \dfrac{\hat{\theta}(x^1, y) + ... + \hat{\theta}(x^m, y)}{m}$.

To apply the ICE method, a definition of an estimator from complete data $\hat{\theta}(X,Y)$ to is necessary –condition (ii)-.

First, we have to compute the parameters of the data attachment term, the (μ, L, M) defining the Fisher distribution of a class. As mentioned in the previous section, the log-cumulant approach can be applied. So knowing a current classification x^k, and the y observed SAR image, for each label value $\omega_i \in \Omega$ we can select the pixels in y for which $x_s^k = \omega_i$ and:

- Estimate the three first log-cumulants using (3.9)-(3.10);
- Compute L^i, M^i and μ^i using (3.8).

Secondly, for the regularization parameters defining the clique potentials, we propose to use the following method which is a least square estimation to estimate the α parameters $(\alpha_H^1, \alpha_V^1, \alpha_{aH}^2, \alpha_{aV}^2, \alpha_{bH}^2, \alpha_{bV}^2)$ defining the Markov distribution of (X,U) (Benboudjema and Pieczynski, 2005) and which can be summarized in the four following steps:

- Find the relationship between the joint probabilities $p(x_s, u_s, x_{V_s}, u_{V_s})$ and the $\alpha = (\alpha_H^1, \alpha_V^1, \alpha_{aH}^2, \alpha_{aV}^2, \alpha_{bH}^2, \alpha_{bV}^2)$ parameter (x_{V_s}, u_{V_s} represent the configuration of X and U in the neighborhood of s;
- Estimate all such probabilities using histogram technique;
- Construct the over-determined system of equations;
- Solve it using the least squares method.

This procedure is fully described in (Benboudjema and Pieczynski, 2005).

4.1 Practical implementation of the algorithm

This section gives practical information for the application of the proposed classification method.

Initialization: This method is unsupervised in the sense that it does not require a supervised learning of the parameters (nor for the data attachment term, neither for the regularization one). Nevertheless, the number of desired classes has to be given as well as some initial values of the parameters to start their estimation.

Concerning the data attachment term, it has been initialized with a k-means algorithm (MacQueen 1967). It is a two steps procedure that iteratively alternates classification and updating of classes. First, some class centers are chosen among the amplitude values. The choice is done by uniform sampling in the interval defined by the minimum value of the radar image and the mean plus three times the standard deviation. Both mean and standard deviation are computed on the whole image. This interval is used instead of the minim – maximum interval to avoid the influence of the bright scatterers in the SAR image. Then a classification step of the amplitude to the closest center is applied. The centers are eventually adjusted by an empirical mean and the process is iterated. These steps (classification and center updating) could be improved for SAR data but it is used only as an initialization algorithm. Based on the final associated classification, the log-cumulant method is used to initialize of the parameters of the Fisher distribution of each class.

Concerning the regularization term, the vector $\alpha = (\alpha_H^1, \alpha_V^1, \alpha_{aH}^2, \alpha_{aV}^2, \alpha_{bH}^2, \alpha_{bV}^2)$ has been initialized with a constant vector $\alpha = (1, 1, 1, 1, 1, 1)$.

Global algorithm: The figure Fig.1 summarizes the different steps of the algorithm. Concerning ICE parameter estimation, only one realisation of X and U according to their distribution conditionally on $Y = y$ and based on θ_n is sampled (meaning that $m = 1$), and 20 ICE iterations are used to obtain the final parameter estimation. Each Gibbs sampler uses 20 updates of the image. For the final classification using the MPM estimator, 100 samples (i.e images of x and u) are drawn to compute the most frequent value in each pixel.

V. EXPERIMENTS AND DISCUSSION

In this section we present two sets of experiments to illustrate the interest of the proposed approach: first using simulated images, and second with real high resolution SAR data.

5.1 Simulated images

This first series of experiments concerns simulated TMF and can be seen as a validation of the proposed approach in an "ideal case". For that, we use the Gibbs sampler algorithm with the energy given by (2.2). Each X_s takes its values in the set of two classes $\Omega = \{\omega_1, \omega_2\}$, and each U_s takes its values in the set of two stationarities $\Lambda = \{a, b\}$, i.e. there are two different homogeneities in the class image $X = x$. The observation image is then sampled using the Fisher distribution whose parameters are presented in Table 1 for the two classes. Then, we use the proposed algorithm to classify the image as described in Section IV. We compare the results with the same algorithm but supposing Gaussian or Gamma distribution.

Figure (2a) represents a simulated image using the TMF model. Figure (2b) is the associated observed image with Fisher's distribution whose values are given in Table 1. The unsupervised MPM result based on Fisher distribution is shown in Figure (2d). This one has been compared with those obtained supposing that the margins of the classes are Gamma and Gaussian represented in Figures (2e) and (2f), respectively. It can be deduced from this experiment and comparisons that it is important to take into account the true distribution of the SAR data, and that the results are strongly improved by the Fisher distribution. These experiments also illustrate that the regularization parameters are better evaluated with a good data attachment term.

5.1 Real SAR images

This subsection is devoted to tests on a real SAR image. A large dataset of images according to its types (high or medium resolution) has been used but only one example is given. The image (2048x2048) used here represents the Bayard district near Dunkerque, France and has been acquired by an aerial sensor of ONERA with a resolution under one meter. We have considered six classes and two values for the U field. Note that this number has been set arbitrarily for the sake of simplicity, but one could use more sophisticated approaches to estimate this number in an automatic way. Results of unsupervised segmentation are shown in Figure 3.

<u>Comparison of TMF and HMF</u>

The results are shown in Figure 3 and Figure 5. In all cases, the results are improved by the TMF compared to the HMF model. The different classes are more regularized and less confusion between the different classes can be observed. The shapes of the different estimated distributions are represented in Figure 6. They represent the mixture of the distributions (Fisher, Gamma and Gaussian) that have been found for the different classes and should approximate the image histogram.

Comparison of Fisher and Gamma distributions

For information we also gave the result with Gaussian distributions but this model is clearly not adapted for SAR images. In fact, the classification obtained using the classical HMF model provided weak results since some regions are fused and others are mixed (see zoom in figure 5). The comparison between Gamma and Fisher distributions leads to the three following remarks:

- results are more regularized with Fisher distributions (see Figure 4)
- Fisher classes are more adapted to urban elements; indeed, the buildings are better segmented with Fisher than with Gamma distribution (predominantly white class, instead of mixing of red and white); besides the classes of the third field U (see Figure 4) have a good coherency corresponding to homogeneous areas (in black) and textured ones (white) in the case of Fisher distribution.
- Gamma and Fisher distributions automatically found by the algorithms do not coincide; we can see that the L parameters found with Fisher distributions are closer to reality (the theoretical value should be 1); besides, as expected, the heavy tailed Fisher distributions have a lower μ parameter than the Gamma distributions (see Table 2).

Interest of the proposed segmentation method for urban areas

In this section, we will consider only the TMF + Fisher method. The following remarks can be made on the results. First, the global results are good; and thus the algorithm proposed could be useful for further applications (registering, 3D reconstruction). The proposed approach has automatically found the salient features of urban landscapes: roads, shadows, buildings, ground and vegetation. Among the limits of the proposed approach, we can see that road and shadows have not been clearly distinguished and that there is a class mixing buildings and vegetation (red class). The point is that these features have very close radiometry. Higher level processing should be introduced to deal with this problem (for instance knowledge on building shapes).

VI. CONCLUSION

In this paper we have presented an original method for unsupervised image segmentation, which is based on the triplet Markov field (TMF) model recently introduced and the Fisher distribution. These models are used in an unsupervised classification algorithm using a parameter estimation method based on Iterative Conditional Estimation (ICE). Experiments indicate that the proposed approach improves the unsupervised image segmentation quality. Indeed, the use of second kind statistics is well adapted to SAR images because they are less sensitive to high values and the use of the TMF model allows the extraction of additional information in the image, namely the field of different local interactions U .

As far as perspectives are concerned, let us notice that different recent hidden Markov field based methods, such as (Picco and Palacio, 2011; Salah et al., 2011), could probably be extended to the more general triplet Markov field based methods. Let us also mention that Markov trees can be used instead of Markov fields to model and process non-stationary images (Liu et al., 2011). Finally, we could possibly extend this study to the triplet Markov chains (Pieczynski, 2010). Investigation of more than 2 "stationarities" to process more extended areas could also be the subject of further work.

REFERENCES

Benboudjema D. and Pieczynski W., 2005, "Unsupervised image segmentation using triplet Markov fields", *Computer Vision and Image Understanding*, Vol. 99, No. 3, pp. 476-498.

Benboudjema D. and Pieczynski W., 2007, "Unsupervised statistical segmentation of non stationary images using triplet Markov fields", *IEEE Transaction on Pattern Analysis and Machine Intelligence*, Vol. 29, No. 8, pp. 1367-1378.

Benboudjema D. Tupin F., Pieczynski W., Sigelle M., and Nicolas J-M., 2007, "Unsupervised statil segmentation of SAR images using Triplet Markov fields and Fisher noise distribution", *IGARSS (IEEE International Geoscience and Remote Sensing Symposium)*, Barcelona, Spain.

Delignon Y., Marzouki Y. and Pieczynski W., 1997, "Estimation of generalized mixture and its application in image segmentation", *IEEE Transaction on Image Processing*, Vol. 6, No. 10, pp. 1364-1375.

Fjortoft R., Delignon Y., Pieczynski W., Sigelle M. and Tupin F., 2003, "Unsupervised segmentation of radar images using hidden Markov chains and hidden random fields", *IEEE Transaction on Geoscience and Remote Sensing*, Vol. 41, No. 3, pp. 675-686.

Gao G., 2010, "Statistical modeling of SAR images: A Survey", *Sensors*, Vol. 10, pp. 775-795.

Geman S. and Geman D., 1984, "Stochastic relaxation, Gibbs distributions and the Bayesian restoration of images", *IEEE Transaction on Pattern Analysis and Machine Intelligence*, Vol. 6, pp. 721-741.

Goodman J.W., 1976, "Some fundamental properties of speckle", *Optical Society America Journal*, Vol. 66, No. 11, pp. 1145-1150.

Gradshteyn I. and Rayzhik I., 2000, "Table of integrals, series and products", *6th edition, A. Jeffrey and D. Zwillinger, Eds. London, U.K. Academic*.

Guyon X., 1995, "Random fields on a network", *Springer-Verlag, Probability and its applications*.

Kuruoglu E.E. and Zeroubia J., 2004, "Modeling SAR images with a generalization of the Rayleigh distribution", *IEEE Transactions on Image Processing*, Vol. 13, No. 4, pp. 527-533.

Liu Y., Wong A., and Fieguth P., 2011, "Synthesis of Remote Sensing Label Fields Using a Tree-Structured Hierarchical Model*", IEEE Transactions on Geoscience and Remote Sensing.*

Lopes A., Touzi R. and Nezry E., 1990, "Adaptative speckle filters and scene heterogeneity", *IEEE Transactions on Geoscience and Remote Sensing,* Vol. 28, No. 6, pp. 992-1000.

MacQueen J., 1967, "Some methods for classification and analysis of multivariate observations", Proceding of Fifth Berkley Symposium on Mathematics Statistics and Probability, Vol. 1, pp. 281-297.

Marques R., Medeiros F., Nobre J., 2012, "SAR image segmentation based on level-set approach and G_A^0 Model", IEEE Trans. On Pattern Analysis and Machine Intelligence, Vol. 34, Num. 10.

Marroquin J., Mitter S. and Poggio T., 1987, "Probabilistic solution of ill-posed problems in computational vision", *Journal of the American Statistical Association*, Vol. 82, No. 397, pp. 76-89.

McLachlan G.J. and Krishnan T., 1997, "EM algorithm and extensions", *Wiley, Series in Probability and Statistics*.

Mignotte M., Collet C., Pérez P. and Bouthémy P., "Sonar image segmentation using an unsupervised hierarchical MRF model", *IEEE Transaction on Image Processing,* Vol. 9, No. 7, pp. 1216-1231, 2000.

Nezry E., Lopes A., Ducrot-Gambart D., Nezry C. and Lee J.-C., 1996, "Supervised classification of K-distributed SAR images of natural targets and probability of error estimation", *IEEE Transaction on Geoscience and Remote Sensing,* Vol. 34, No. 5, pp. 1233-1242.

Nicolas J.-M., 2006, "Application de la transformée de Mellin : étude des lois statistiques de l'imagerie cohérente", *Note technique ENST 2006D010*.

Oliver C.J., 1984, "A model for non-Rayleigh scattering statistics", *Journal of Modern Optics*, Vol. 31, No. 6, pp. 701-722.

Pellizzeri T.M., Gamba P., Lombardo P. and Dell'Acqua F., 2003, "Multitemporal/multiband SAR classification of urban areas using spatial analysis: statistical versus neural kernel-based approach", *IEEE Transaction on Geoscience and Remote Sensing,* Vol. 41, No. 10, pp. 2338-2353.

Pérez P., "Markov random fields and images", *CWI Quarterly*, Vol. 11, No. 4, pp. 413-437, 1998.

Picco M. and Palacio G., "Unsupervised classification of SAR images using Markov random fields and G_I^0 model", *Geoscience and Remote Sensing Letters*, Vol. 8, No. 2, pp. 350-353, 2011.

Pieczynski W., 1992., "Statistical image segmentation", *Machine Graphics and vision*, Vol. 1, No. 1, pp. 261-268.

Pieczynski W. and Benboudjema D., "Multisensor triplet Markov fields and theory of evidence", *Image and Vision Computing*, Vol. 24, No. 1, pp. 61-69, 2006.

Pieczynski W., Triplet Markov chains and image segmentation, chapter 4 in Inverse problems in Vision and 3D Tomography, A. Mohammed-Djafari ed., *Wiley*, 2010.

Reed S., Petillot Y. and Bell J., "An automatic approach to the detection and extraction of mine features in sidescan sonar*", IEEE Journal of Oceanic Engineering*, Vol. 28, No. 1, pp. 90-105, 2003.

Salah M.B., Mitiche A., and Ayed I.B., "Multiregion image segmentation by parametric kernel graph cuts", *IEEE Transaction on Image Processing*, Vol. 20, No. 2, pp. 545-557, 2011.

Tison C., Nicolas J.M., Tupin F., Maître H., "A New Statistical Model for Markovian Classification of Urban Areas in High Resolution SAR Images*", IEEE Transaction Geoscience and Remote Sensing*, Vol. 42, No. 10, pp. 2046-2057, 2004.

Tison C., Tupin F. and Maitre H., "A fusion scheme for joint retrieval of urban map and classification from high resolution interferometric SAR images", *IEEE Transaction on Geoscience and Remote Sensing*, Vol. 45, No. 2, pp. 496-505, 2007.

Winkler G., "Image analysis, random fields and Markov chain Monte Carlo methods: a mathematical introduction", *Springer*, 2003.

Won C.S. and Gray R.M., "Stochastic images processing", *Kluwer Academic / Plenum Publishers*, New York, 2004.

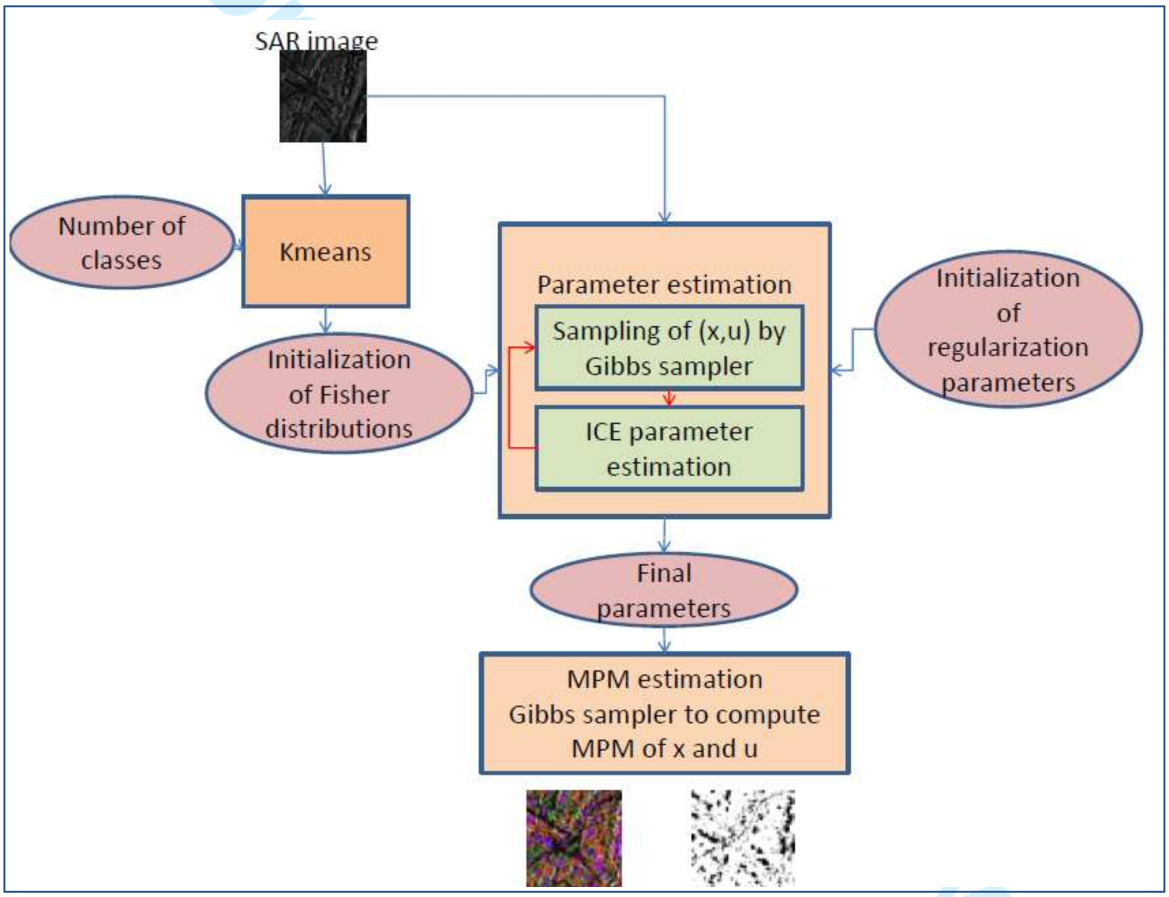

Figure 1. Overview of the unsupervised segmentation algorithm and its different steps.

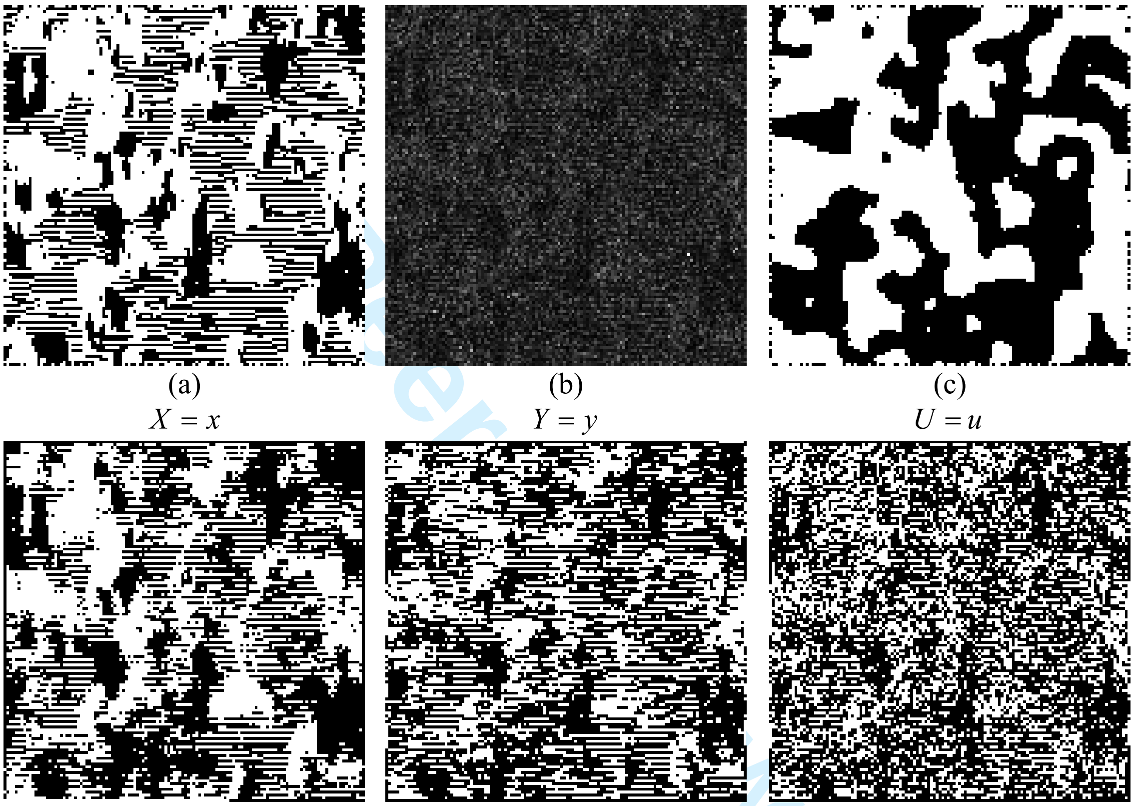

(a) $X = x$ (b) $Y = y$ (c) $U = u$

(d) Fisher 20.33% (e) Gamma 24.52% (f) Gaussian 30.52%

Figure 2. Simulated image using TMF model and MPM segmentation results based on (d) Fisher distribution, (e) Gamma distribution and (f) Gaussian distribution. The indicated percentage

Bayard – original SAR image

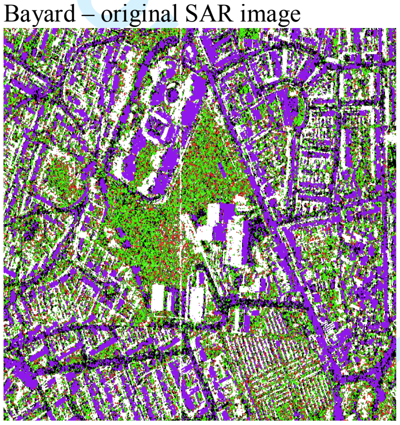

Estimated X using HMF+Fisher

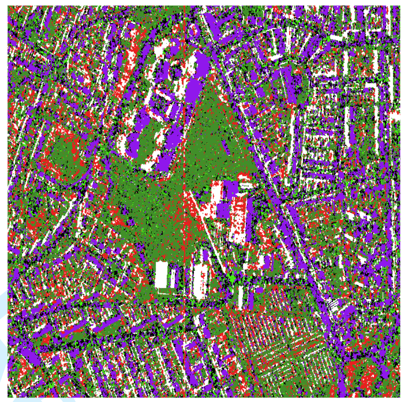

Estimated X using TMF+Fisher

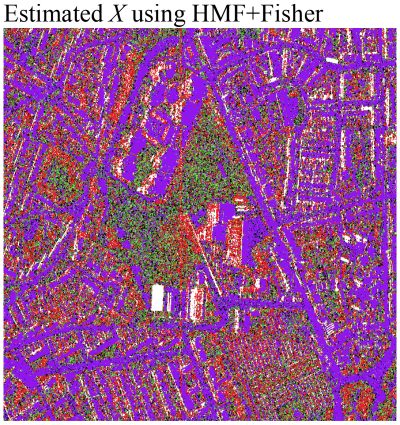

Estimated X using HMF+Gamma

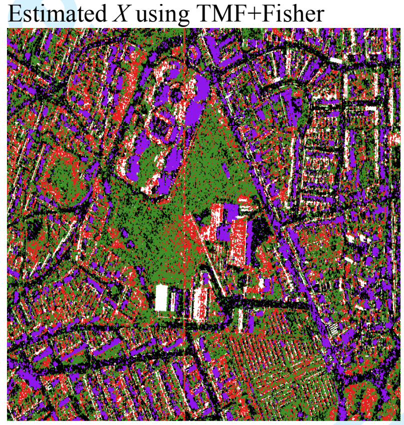

Estimated X using TMF+Gamma

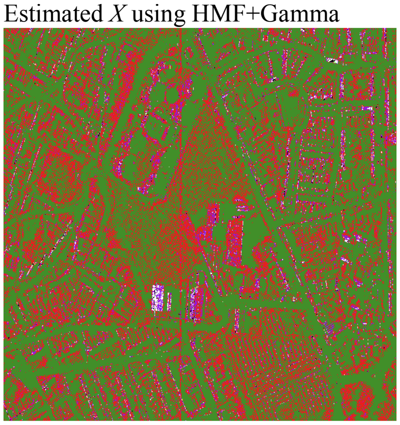

Estimated X using HMF+Gaussian

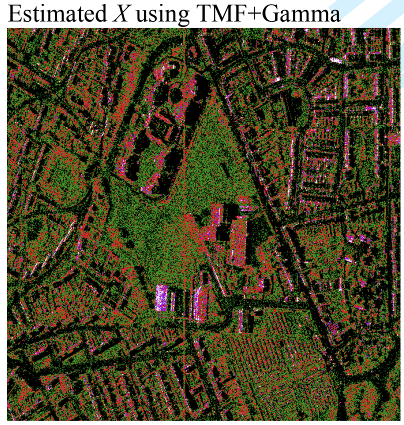

Estimated X using TMF+Gaussian

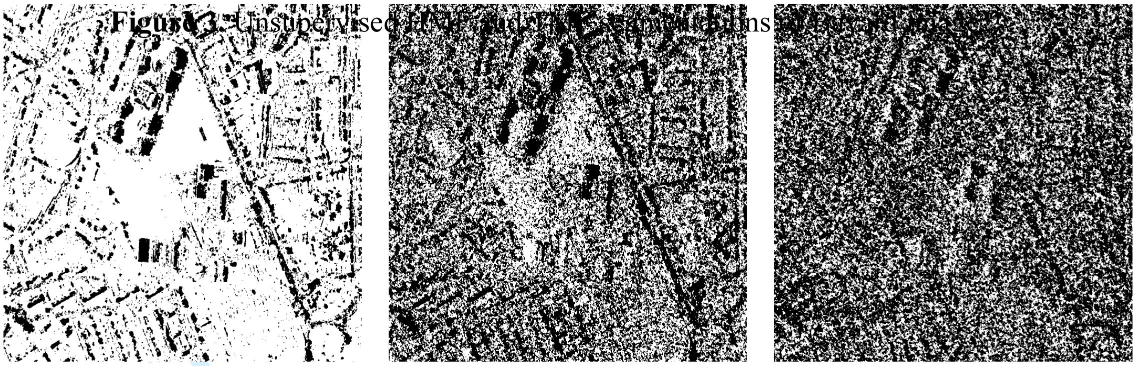

Using Fisher distribution Using Gamma distribution Using Gaussian distribution

Figure 4. Estimated U corresponding to figure 3 using TMF model.

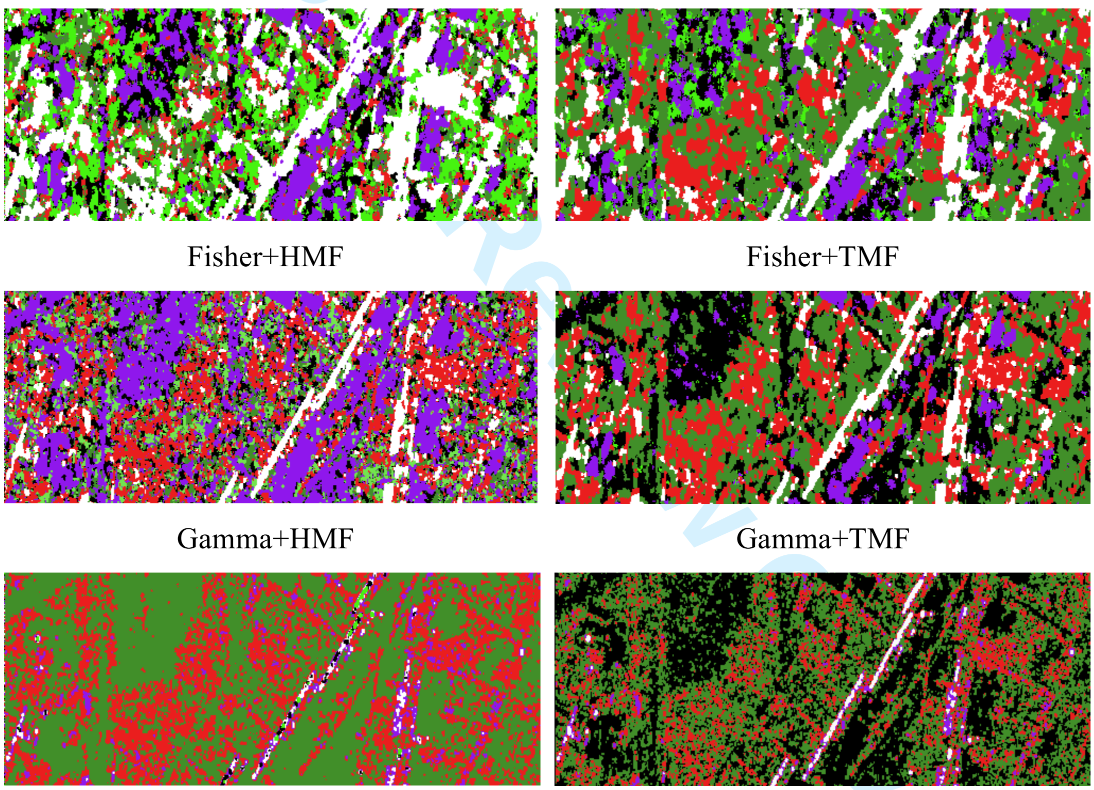

Fisher+HMF Fisher+TMF

Gamma+HMF Gamma+TMF

Gaussian+HMF Gaussian+TMF

Figure 5. Zoom of the same region corresponding to figure 3.

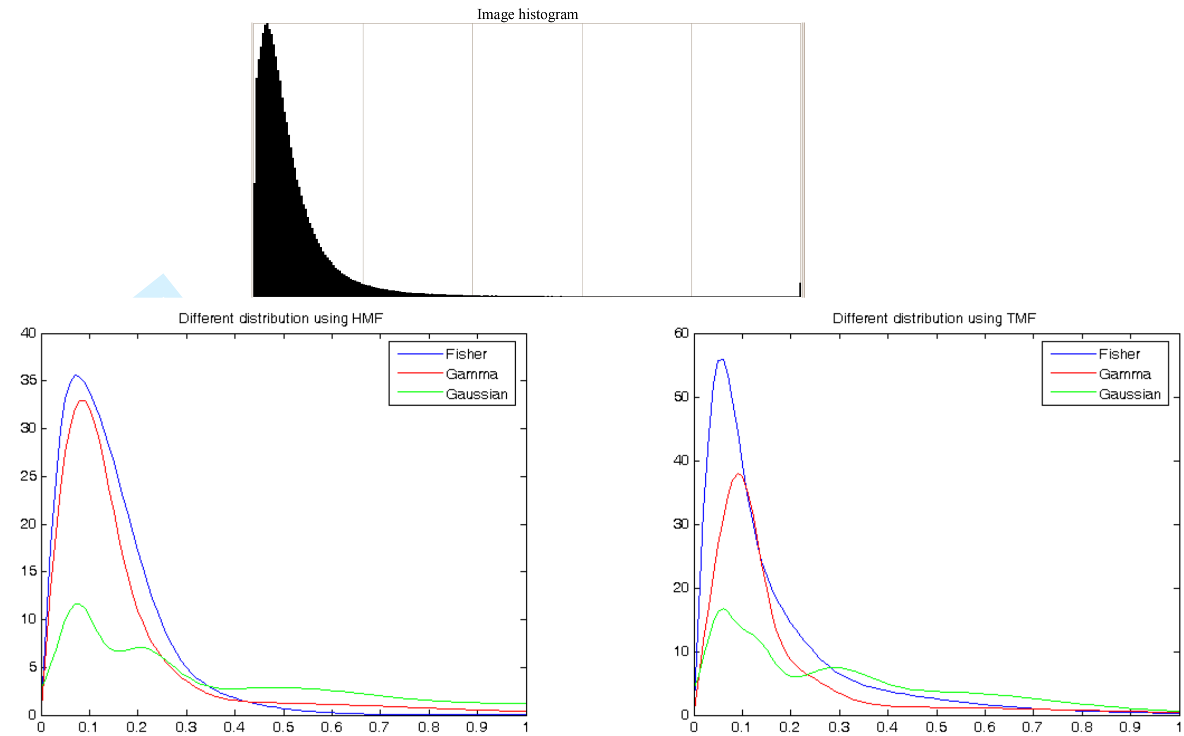

Figure 6. Mixture of the estimated Fisher, Gamma and Gaussian pdfs in the (left) HMF model, (right) TMF model and (top) Image histogram. The amplitude axis has been re-sampled between 0 and 1, 1 being the mean plus three times the standard deviation of the image.

Parameters	Real values	Fisher	Gamma	Gaussian
α_H^1, α_V^1	1., 1.	1.06, 0.99	0.89, 0.89	0.83, 0.94
$\alpha_{aH}^2, \alpha_{aV}^2$	1., -0.3	0.79, -0.2	0.75, -0.11	0.35, -0.12
$\alpha_{bH}^2, \alpha_{bV}^2$	0.3, 1.	0.3, 0.72	0.32, 0.44	0.19, 0.24
μ_1, μ_2	5., 10.	5.68, 9.31	6.20, 11.1	4.60, 10.77
M_1, M_2	3., 10.	2.33, 5.75	-	-
L_1, L_2	1., 1.	1.02, 1.01	0.93, 0.94	-
σ_1, σ_2	-	-	-	2.23, 5.07
Error ratio		20.33%	24.52%	30.52%

Table 1. Estimated parameters and unsupervised segmentation results using different distributions.

Parameters	Gamma	Fisher
L	0.97, 1.79, 1.79, 1.13, 1.49, 0.84	0.98, 1.26, 1.03, 1.12, 1.21, 1.06
M	-	6.7, 26.65, 31.65, 39.37, 28.47, 5.72
μ	0.06, 0.09, 0.11, 0.13, 0.22, 0.65	0.05, 0.07, 0.08, 0.09, 0.17, 0.25

Table 2. Estimated parameters corresponding to Gamma and Fisher distributions.